JOURNAL OF MATERIALS SCIENCE 39 (2004) 6901–6908

Fatigue behavior of AISI 347 stainless steel in various environments

CHIH-KUANG LIN*, I-LON LAN
Department of Mechanical Engineering, National Central University, Chung-Li 32054, Taiwan
E-mail: t330014@cc.ncu.edu.tw

The aim of this study is to investigate the influence of environmental factors, including pH, chloride ion, and pitting inhibitor, on the fatigue properties of AISI 347 stainless steel. Systematic fatigue tests, including both high-cycle fatigue (HCF, S-N curves) and fatigue crack growth (FCG, da/dN-ΔK curves), have been conducted in air and several aqueous environments. Results showed the HCF strength was markedly reduced in an acid solution and in a chloride-containing solution, as compared to the air value. An addition of pitting inhibitor could restore the HCF strength in salt water back to the level in atmospheric air by preventing the formation of corrosion pits and decreasing the corrosion rate. However, the corresponding stage II FCG rates in all given environments were almost equivalent. These results indicated that the variation of chemistry in bulk environment exerted more influence on the fatigue crack nucleation than on the extension of long fatigue cracks.

1. Introduction

AISI 347 stainless steel (SS) was developed to improve the resistance of 304 austenitic SS to intergranular stress corrosion cracking (IGSCC) by adding niobium (Nb) to form niobium carbides in preference to Cr-rich carbides so that the depletion of chromium at grain boundary regions could be reduced [1]. Most of the previous studies related to AISI 347 SS were mainly focused on microstructural characterizations [2, 3], corrosion properties [4, 5], sensitized degradation [6, 7], hydrogen embrittlement [8–11], creep [12–14], and high-temperature brittle fracture [15, 16]. However, only limited work has been done on the fatigue strength of AISI 347 SS [17] and there is still lack of systematic studies on the corrosion fatigue (CF) properties of 347 austenitic SS. Although most of the applications of this austenitic SS are subjected to static loading, some of the applications are involved with cyclic loading. As the fracture behavior under cyclic loading in aggressive environments might be different from the one under static loading, it is important to study the CF properties of AISI 347 SS so as to better assess and predict the service life of the components made of this alloy. The present work was therefore planned to characterize the environmental effects on the fatigue crack initiation and propagation stages in AISI 347 by conducting systematic experiments, including both high-cycle fatigue (HCF) and fatigue crack growth (FCG), in air and several aqueous environments, including deionized water, H_2SO_4, NaCl and inhibited NaCl solutions. Hopefully, the experimental CF data of the current study will provide some insight into fatigue behavior of 347 SS in various environments for development of fatigue design methodology of AISI 347 components.

2. Experimental procedures

The chemical composition of the as-received 347 SS used in the current study is given in Table I. The alloy was supplied by the vendor in the form of round bars of 12.7 and 88.9 mm diameter. The small and large round bars were used to fabricate HCF and FCG test specimens, respectively. The specimens were heat-treated at 1050°C for 1 h and then water quenched to obtain a solution-annealed condition of which the mechanical properties have an ultimate tensile strength of 658 MPa, a yield strength of 310 MPa, an elastic modulus of 190 GPa, an elongation of 61.4% (in 25 mm), and a hardness value of 42 HRb.

Both HCF and FCG tests were carried out at room temperature in laboratory air and four aerated aqueous environments: (1) deionized water (pH = 6.3); (2) 50 ppm H_2SO_4 solution (pH = 3.0); (3) 3.5 wt% NaCl solution (pH = 6.1); (4) 3.5 wt% NaCl + 3000 ppm methoxypropylamine (MPA) solution (pH = 11.1). All solutions were prepared from distilled deionized water. The sulfuric acid solution was used for a general corrosion condition while the salt water was used for evaluating the pitting corrosion resistance of AISI 347.

*Author to whom all correspondence should be addressed.

TABLE I Nominal chemical composition of AISI 347 SS (wt%)

Cr	Ni	Mn	Nb	Si	Mo	Cu	Co	C	N	S	P	Ta	Fe
17.28	10.23	1.67	0.63	0.59	0.09	0.08	0.05	0.05	0.035	0.025	0.023	<0.01	Bal.

The addition of MPA in NaCl solution was used to study the effect of pitting inhibitor on the CF properties of the given alloy. All CF tests were conducted under freely corroding conditions, i.e., no external potential was applied to the specimens. HCF tests were conducted as per ASTM E466 on axial smooth-surface specimens, with a cylindrical gage section of 6 mm in diameter and 18 mm in length, to determine the stress-life (S-N) curves. FCG experiments were performed in accordance with ASTM E647 on 6.35-mm-thick compact tension (CT) specimens to determine the fatigue crack growth rate (FCGR) curves in terms of da/dN-ΔK relationship. Both types of specimens were machined with the fatigue loading direction parallel to the axial direction of the initial round bars. Details of the specimen geometry and experimental set-up for such CF tests were described elsewhere [18]. All fatigue tests were performed on a closed-loop, servohydraulic machine under a sinusoidal loading wave form with a load ratio of R (minimum load/maximum load) = 0.1 and a frequency of $f = 5$ Hz. The HCF tests were run to failure or to 10^6 cycles where specimen was considered to be a runout. All CT specimens were first fatigue precracked in laboratory air before testing in the aqueous environments. The crack length in the FCG test was determined by a compliance technique recommended by ASTM E647 using a clip gage mounted on the front edge of the CT specimen to monitor the crack-mouth-opening displacement during testing. Characterizations of the fracture surface morphology were made by scanning electron microscopy (SEM).

Two types of electrochemical measurements were also conducted to obtain the polarization characteristics for the given alloy-aqueous-environment systems. Specimens with an exposed area of $\sim$1 cm^2 were mounted in chemical resistant epoxy resin to form the working electrode. Anodic polarization curves in each given aqueous environment were obtained with a potentiodynamic polarization technique using a commercial corrosion measurement instrument at a scan rate of 1 mV/s. The corrosion potential (E_{corr}) and pitting potential (E_{pit}) for each given alloy-aqueous-environment system were thus determined from these anodic polarization curves. Note that all potentials were measured with reference to a saturated calomel electrode (SCE) and platinum wires were used as the counter electrodes. Another type of measurement in obtaining the anodic and cathodic polarization curves at the linear Tafel region was also applied to assess the corrosion rate (I_{corr}, corrosion current density) in each alloy-aqueous-environment system by extrapolation of the anodic and cathodic Tafel slopes. Details of these typical electrochemical measurement techniques can be found in Ref. [19].

3. Results and discussion

3.1. Electrochemical polarization characteristics

Typical potentiodynamic polarization curves for AISI 347 SS in different, aerated aqueous solutions are shown in Fig. 1. The active, passive and transpassive ranges in sequence with rising potential were observed in each case. For metals that exhibit passive behavior, the potential at which passivity breaks down with increasing applied potential is defined as the pitting potential, E_{pit}. The more positive the value of E_{pit}, the more oxidizing conditions that the alloy can withstand prior to the onset of pitting. The values of E_{pit} and E_{corr} determined from these curves are listed in Table II. Note that the fatigue strength data for each given environment are also listed in Table II and will be discussed in next section. The values of corrosion current density (I_{corr}) determined from extrapolation of Tafel slopes for each given aqueous medium are also present in Table II.

By using the results of deionized water as baseline data for comparison, it is clear in Fig. 1 that the E_{pit} value was lowered with a decrease in solution pH (such as H_2SO_4 solution) or with a presence of Cl^- ion (such as NaCl solution). In particular, the pitting resistance of the given alloy was significantly reduced in the NaCl solution. This is expected as chloride is usually present as an essential ingredient to break down the passive film and initiate localized corrosion. It can also be seen in Table II that I_{corr} was increased from 0.107 μA/cm^2 in deionized water to 0.246 μA/cm^2 in NaCl solution and to 0.641 μA/cm^2 in H_2SO_4 solution. The higher

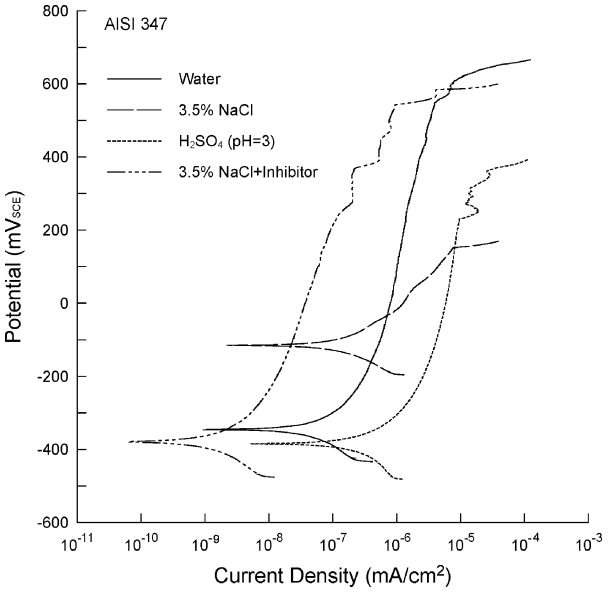

Figure 1 Potentiodynamic polarization curves for AISI 347 SS in different environments.

TABLE II Polarization data and fatigue strength for AISI 347 SS in different environments

Environment	E_{corr} (mV_{SCE})	E_{pit} (mV_{SCE})	I_{corr} ($\mu A/cm^2$)	Fatigue strength at 10^6 cycles (MPa)	Fatigue strength ratio
Air	–	–	–	182	1
Deionized water, pH = 6.3	−346	542	0.107	179	0.98
3.5 wt% NaCl, pH = 6.1	−115	146	0.246	140	0.77
50 ppm H_2SO_4, pH = 3.0	−385	363	0.641	111	0.61
3.5 wt% NaCl + 3000 ppm MPA, pH = 11.1	−379	595	0.005	191	1.05

corrosion rate observed in the H_2SO_4 solution could be attributed to the fact that the passive film is thin and less protective in an acid medium as the oxide is more soluble due to the enhanced activity of hydrogen ions. By adding 3000 ppm MPA into the 3.5% NaCl solution, the corrosion resistance of AISI 347 SS in salt water was significantly improved, as the E_{pit} was considerably increased from 146 to 595 mV_{SCE}. The corrosion rate was also significantly decreased on the addition of MPA as the pH was increased from 6.3 to 11.1 to prompt formation of a more protective film. Therefore, MPA did serve as an effective corrosion inhibitor for the given alloy in salt water. This is because MPA is a type of adsorption inhibitor which controls corrosion through chemisorption onto metal oxide or oxide free surfaces to form a protection barrier [5].

3.2. Fatigue behavior in various aqueous environments

Fig. 2 shows the S-N curves for the smooth-surface HCF specimens tested in air, deionized water, 3.5% NaCl solution and 50 ppm H_2SO_4 solution. The straight solid and dash lines in Fig. 2 represent the best-fit S-N curves. The estimated fatigue strengths corresponding to 10^6 cycles for each environment are given in Table II in which the air value was used as the baseline data to determine the relative fatigue strength ratio in other aqueous environments. Fig. 2 clearly demonstrates deleterious effects of the three uninhibited aqueous environments on the HCF response of AISI 347 SS, as a marked reduction of fatigue life was found in each aqueous solution compared to atmospheric air,

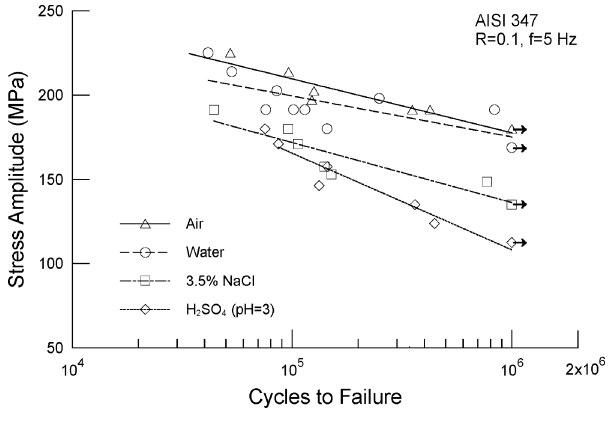

Figure 2 S-N curves for AISI 347 SS tested in different environments. (Arrows designate runout tests.)

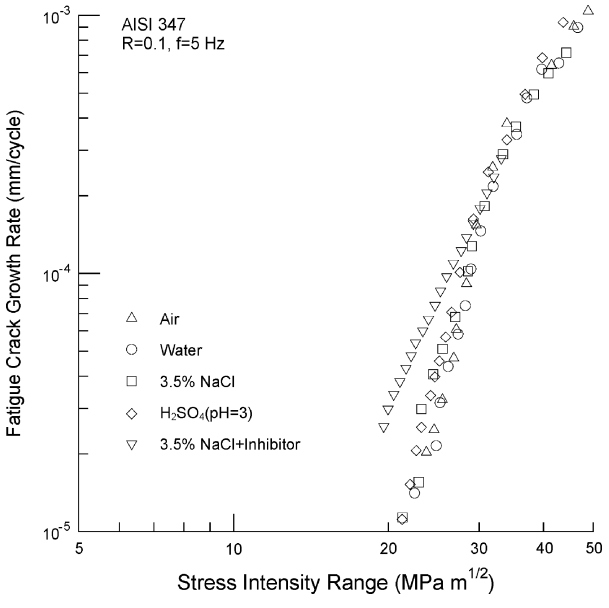

Figure 3 Fatigue crack growth rate curves for AISI 347 SS tested in different environments.

in particular for the salt water and sulfuric acid solution. The counterpart results of the FCG tests using pre-cracked CT specimens were plotted as (da/dN) vs. (ΔK) in Fig. 3 where FCGRs in air were not significantly different from those in the given three uninhibited aqueous media. Apparently, these three uninhibited aqueous media did not generate as severe damage on the FCG resistance of pre-cracked CT specimen (stage II cracking only) as they did in the case of smooth-surface HCF specimen (including crack initiation, stage I and stage II cracking) under a cyclic load of 5 Hz. In this way, S-N curve comparison provided a good indication of the effect of environment on fatigue crack initiation. Note that any results related to the environment of 3.5% NaCl + 3000 ppm MPA solution will be discussed in next section to describe the effect of inhibitor on the CF resistance of 347 SS.

The above comparisons between HCF and FCG results showed the HCF life depended primarily on crack nucleation stage and the environmental effect on the CF resistance of 347 SS was exerted mainly on the phase of crack initiation and stage I crack growth rather than on the phase of stage II crack growth. Similar trends have also been found for other grades of steels and stainless steels [20–22] in which the fatigue lifetime in an aggressive environment was controlled by early growth of initial defects or short cracks of

microstructural dimensions. Although several CF processes may take place throughout the lifetime, the controlling ones are those that strongly depend on the interaction between cyclic stresses and aggressive environment which often leads to strain localization and enhanced growth of defects and short cracks [20]. These governing processes include pitting, preferential dissolution, stage I crack growth and transition from stage I-to-stage II crack growth [20]. It was generally recognized that corrosion pits and/or accelerated dissolution at emerging slip steps or extrusion, somehow induced by CF process, prematurely initiate fatigue cracking or reduce the applied stress required to initiate fatigue cracks [20, 23, 24].

Typical fracture surface morphology near the origins of fatigue cracks in HCF specimens is given in Fig. 4. Although these micrographs indicate fatigue cracks generally initiated at the surface in all given environments, different surface features at crack initiation sites were observed. As shown in Fig. 4a and e, no evidence of visible corrosion-induced damages on the surface passive film at fracture origin was found for the specimens tested in the atmospheric air and 3.5% NaCl + 3000 ppm MPA solution. However, fatigue cracks in deionized water, sulfuric acid solution, and sodium chloride solution appeared to initiate from different types of corrosion-induced damages on the surface passive film, as shown in Fig. 4b–d. Breakdown of passive film seems to take place locally at the crack initiation areas for the specimens tested in deionized water and sulfuric acid solution, as shown in Fig. 4b and c, indicating the metal-dissolution behavior for the given alloy in these two aqueous media is likely to be preferential dissolution over pitting corrosion. However, corrosion pits penetrating from surface were indeed observed at the fracture origins on the specimens tested in salt water as exemplified by the label *p* in Fig. 4d. Note that the AISI 347 SS shows the lowest E_{pit} value and pitting resistance in the uninhibited salt water among the given aqueous environments, as indicated in Table II. Even though the formation of corrosion pits might generate certain extent of stress concentration effect to facilitate microcrack development, the growth of these corrosion pits to become short cracks (stage I cracking)

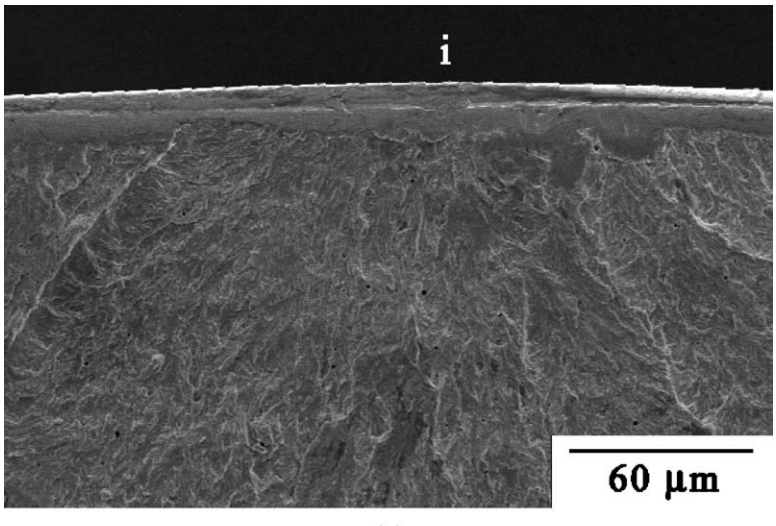

(a)

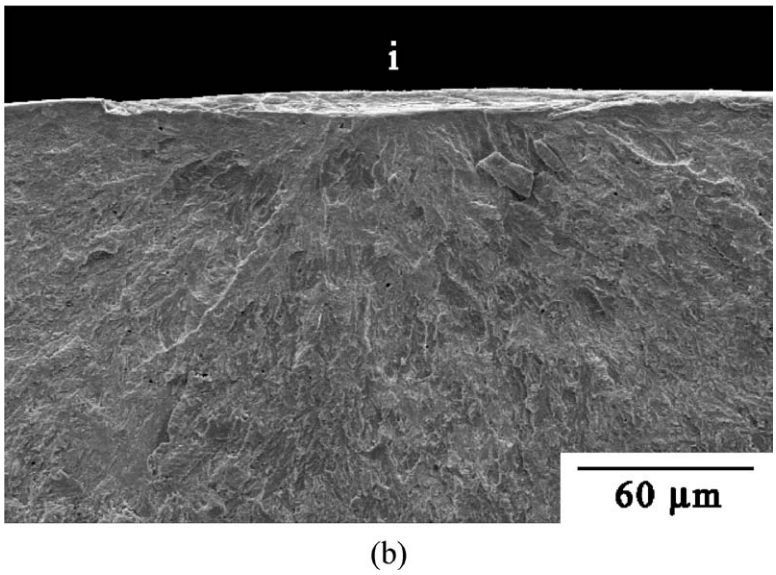

(b)

Figure 4 SEM fractography of HCF specimens of AISI 347 SS tested in different environments: (a) air, (b) deionized water, (c) 50 ppm H_2SO_4 solution, (d) 3.5% NaCl solution, and (e) 3.5% NaCl + 3000 MPA solution. (i: crack initiation site; p: corrosion pit.) (*Continued*.)

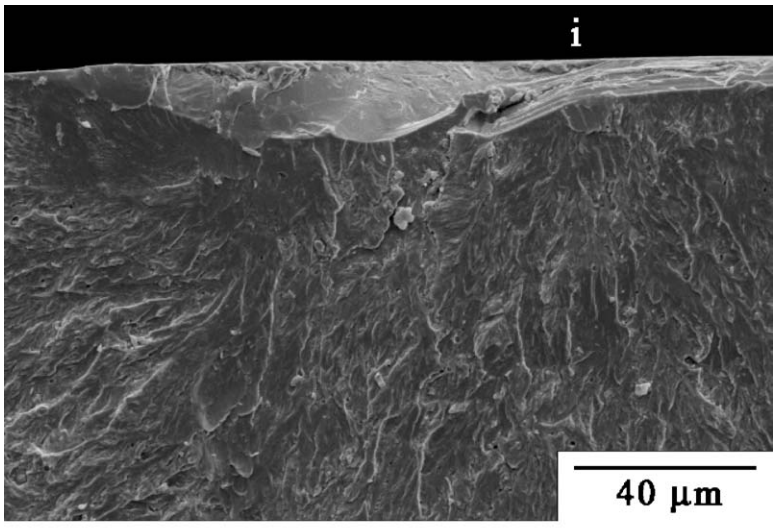

(c)

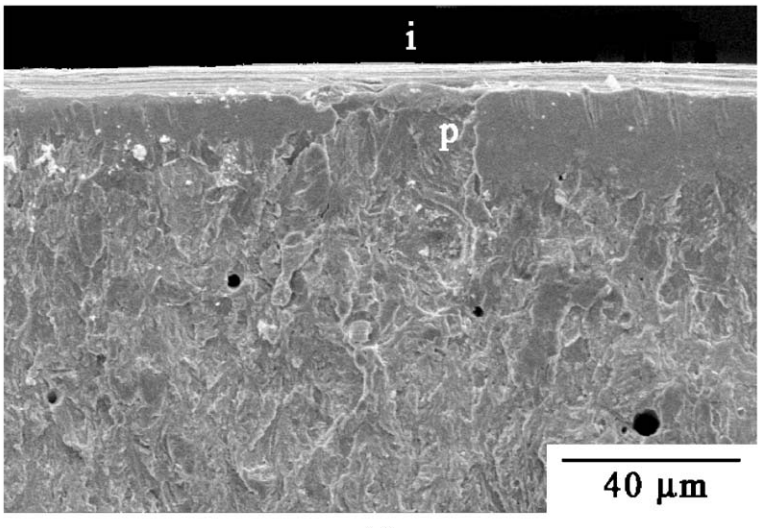

(d)

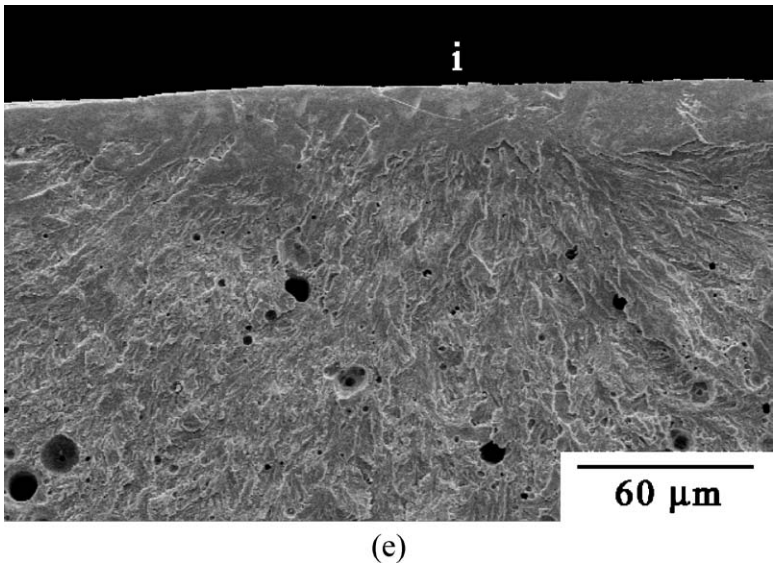

(e)

Figure 4 (*Continued*).

in uninhibited salt water, apparently, was more difficult than that of the corrosion-induced damages with breakdown of surface passive film on specimen tested in sulfuric acid solution. This implied that the stage I cracking of AISI 347 SS in aqueous environments was most likely to be controlled by preferential dissolution at slip bands due to film rupture. This is supported by the fact that the HCF life was markedly shorter in

sulfuric acid solution than in salt water. Therefore, the distinct reduction of HCF life in AISI 347 to different extents by the three given uninhibited aqueous solutions over the atmospheric air could be attributed to an accelerated crack initiation and stage I crack growth caused by preferential dissolution mechanism.

Note that the fatigue cracks grew transgranularly in all given environments as shown in Fig. 4. There were also a few pitting holes (black round spots in Fig. 4d and e) observed at the subcritical crack growth regions on the crack surfaces of the specimens tested in NaCl and NaCl + MPA solutions. In general, these pitting holes formed on the crack surfaces behind the crack tip were only observed in the chloride-containing solutions due to a localized acidification effect within crack. They were not involved in the crack initiation stage, which dominated the HCF life for the given alloy-environment systems. More discussion on the formation of these pitting holes on crack surfaces behind crack tip even in the solution containing pitting inhibitor will be given in next section.

The degree of the environmental effect on the HCF resistance of 347 SS is indeed related to the nature of the corrosive environment. As shown in Fig. 2, among the given three uninhibited aqueous solutions, sulfuric acid solution is the most aggressive in reducing the HCF resistance, followed by the salt water and little deleterious effect was generated by deionized water on the HCF strength. This is consistent with the electrochemical data presented in Table II, where AISI 347 showed the highest corrosion rate in sulfuric acid solution. The higher corrosion rate of AISI 347 in sulfuric acid solution over salt water and deionized water can be attributed to an increase in the hydrogen ion concentration and then an increase in metal dissolution. In this regard, the controlling CF mechanisms such as preferential dissolution at slip bands in an acid medium would be more active in assisting the surface fatigue crack nuclei to overcome the microstructural barriers and accelerate the initial growth. Table II also shows, due to the presence of chloride, salt water is more aggressive than deionized water which explains why the fatigue strength was considerably lower in salt water than in deionized water.

The lack of distinctly corrosive effect from the given three uninhibited aqueous media on the growth of long fatigue crack, when compared to air environment (Fig. 3), indicates that the controlling fracture mechanism might be different between the crack nucleation and propagation stages. As described above, preferential dissolution presumably played a very important role in determining the length of fatigue crack nucleation period and then the entire HCF life. However, this might not be the case for the extension of a long fatigue crack; otherwise the FCGR would have shown differences in the given environments as shown in the HCF results. It is generally believed that the hydrogen embrittlement (HE) and active path dissolution at crack tip are the two typical mechanisms responsible for the enhanced crack growth in an aggressive environment. If preferential dissolution at crack tip were the controlling mechanism for stage II cracking, like the S-N curve results, 5 Hz cyclic loading could have generated differences in detrimental effects on the FCG behavior in these three uninhibited aqueous environments according to the corrosion rate data in Table II. It is therefore inferred that HE is likely to be the controlling mechanism for FCG of 347 austenitic SS in aqueous environments, if it exists. However, the comparable FCGRs observed in the air and three uninhibited aqueous environments implied that a loading frequency of 5 Hz might be too high to distinguish the degree of severity of HE effect on extension of long fatigue crack between the humid air and aqueous environments for the given AISI 347 SS. Note that the relative humidity of the given ambient air was about 60%.

The environmentally-assisted-cracking (EAC) by HE generally involves several sequential processes including transport of deleterious species or environment to the crack tip; chemical/electrochemical reactions at the crack tip in production of hydrogen; hydrogen diffusion and distribution within the crack-tip microstructure; and the embrittlement process itself [25]. The EAC part of FCG is controlled by the slowest process in this sequence and the overall crack growth response is governed by one or more of these processes in conjunction with the mechanical driving force for crack growth [25]. In the current study, the slowest step in the HE sequence could not be determined based on the available data. It is highly possible that under a cyclic load of 5 Hz, the water vapor pressure level in the given humid air and the three given uninhibited aqueous solutions generated no distinct HE effects on control of the FCG behavior leading to comparable FCGRs in the current study.

It was initially, also assumed that the less deleterious effects of the aggressive aqueous environments on the FCG response might be attributed in part to the retardation of crack growth caused by a corrosion-products-induced crack closure effect. However, no significant differences in the crack closure levels could be detected for the CT specimens tested in the ambient air and three given uninhibited aqueous solutions, and similar trends of FCG response in Fig. 3 would be seen if the FCGRs were plotted in terms of effective stress intensity range, ΔK_{eff}, instead of the applied stress intensity range, ΔK. Apparently, for the given cyclic loading conditions, the given three uninhibited aqueous solutions did not produce the same damaging effects on the fatigue resistance of a long crack as it did on the smooth surface for the given alloy.

3.3. Effects of inhibitor on the corrosion fatigue response

Fig. 5 shows the comparison of S-N curves in the environments of ambient air, 3.5% NaCl solution, and 3.5% NaCl + 3000 ppm MPA solution. The addition of 3000 ppm MPA significantly increased the HCF lifetime of AISI 347 from the value in salt water, under a given cyclic stress level. Moreover, the HCF strength at the long life regime (say around 10^6 cycles) in the inhibited salt water was even greater than that in ambient air indicating that 3000 ppm MPA could effectively

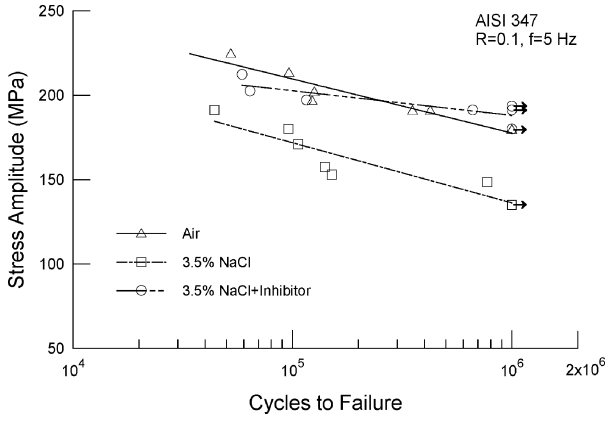

Figure 5 Comparison of S-N curves for AISI 347 SS tested in air and different salt water environments. (Arrows designate runout tests.)

control premature crack initiation that was accelerated by the synergism between the aggressive salt water and the cyclic stresses. SEM micrograph in Fig. 4e also showed that no corrosion-induced damages on the surface passive film at fracture origin were found for specimens tested in 3.5% NaCl + 3000 ppm MPA solution, like the fractography feature in atmospheric air (Fig. 4a). Electrochemical data in Table II also indicated that an addition of 3000 ppm MPA could make the salt water become an alkaline environment, significantly increase the pitting resistance and reduce the corrosion rate to a very low value. As discussed in the previous section, preferential dissolution at slip bands was considered as the controlling mechanism for HCF crack initiation and lifetime. Therefore, addition of 3000 ppm MPA not only provided a means to prevent any formation of corrosion-induced surface defects (e.g., corrosion pits) from serving as premature crack initiation sites in salt water but also minimized the activity of preferential dissolution at slip bands such that the crack nucleation was retarded and the fatigue life was extended.

On the contrary, the FCGRs shown in Fig. 3 indicated that addition of 3000 ppm MPA did not produce any beneficial effect on the stage II cracking resistance in salt water. The FCGRs in 3.5% NaCl + 3000 ppm MPA solution were comparable with (at high ΔK region) or even slightly higher than (at low ΔK region) those in other given environments. The slightly higher FCGRs at low ΔK region in inhibited salt water over the other environments might be attributed to a lesser crack closure effect, as corrosive products which were present on the fracture surfaces of CT specimens tested in other given environments were barely observed in salt water added with MPA. As ΔK decreased, the crack tip opening became smaller and corrosive debris may wedge in the crack-tip region and enhance crack closure to reduce FCGR. Consistent trends from other work [26, 27] also demonstrated an enhanced closure effect induced by oxide/corrosion debris, particularly at low ΔK region, in a more corrosive environment as compared to a less corrosive one.

As described in the previous section, a few corrosion pits were found on the crack surfaces away from the fatigue crack origins even in the 3.5% NaCl + 3000 ppm MPA solution. Although this inhibitor-containing bulk solution is an alkaline solution, the pitting holes were still formed on the crack surfaces behind the crack tip. It is highly possible that once a surface fatigue crack grew to a certain size, the solution within the surface crack became more occluded and prompt localized acidification through dissolution of Fe and subsequent hydrolysis resulting in an acid solution containing chloride within the crack. It has been reported by Brown and co-workers [28, 29] that under freely corroding conditions, crack-tip pH can be highly acidic (pH $\approx$ 3.8) in Fe-based alloys for different bulk solutions with pH between 1 and 10 [28, 29]. The solution within the crack-tip region could become acidified by the dissolution of Fe and subsequent hydrolysis. The activities of pitting corrosion were enhanced when the pH of an aqueous sodium chloride solution was reduced to a significantly acid level. Therefore, it is no surprise that corrosion pits were found on the crack surfaces at subcritical crack growth regions for HCF specimens tested in the inhibited salt water. As these corrosion pits formed away from the crack initiation sites and behind the crack tip were not involved in the crack initiation or stage II crack extension, HCF lifetime should not be influenced by these behind crack-tip corrosion pits. On the other hand, these corrosion pits formed on the crack surfaces did provide strong support for the premise that the solution at the crack-tip region could become acidified regardless of the pH and ion species in the bulk solution.

The overall comparison of the HCF and FCG response of AISI 347 to the addition of 3000 MPA in salt water indicated that this adsorption type of inhibitor was effective as an inhibitor for pitting corrosion on smooth surface as well as for premature crack nucleation through preferential dissolution mechanism but not for stage II cracking. Therefore, selection of an inhibitor for CF needs to clarify the usage for a smooth surface or for a long crack because the dominant mechanisms for fatigue crack nucleation and propagation stages might be different.

4. Conclusions

(1) The HCF life of AISI 347 austenitic SS was dominated by crack initiation stage which was more susceptible to the variation of bulk environment than the phase of stage II crack growth, as the HCF lifetimes were distinctly shortened in salt water and sulfuric acid solution relative to the ambient air values while the corresponding stage II FCGRs were of no significant difference for all given environments.

(2) The degree of detrimentally environmental effect on the HCF response in the given uninhibited aqueous media was of the order: sulfuric acid solution > salt water > deionized water. This was consistent with the trend of corrosion rate in metal dissolution suggesting that preferential dissolution at slip bands play an important role in facilitating premature fatigue crack initiation and reducing the HCF life.

(3) Comparable FCGRs observed in all given environments imply a loading frequency of 5 Hz might be too high to distinguish the degree of severity of hydrogen embrittlement effect on extension of long fatigue crack between the ambient air and aqueous environments for the given AISI 347 SS.

(4) Addition of a pitting inhibitor, 3000 ppm MPA, has been demonstrated to be effective to prevent premature fatigue crack initiation in salt water for AISI 347 SS and extend the HCF life, but not for stage II crack growth.

Acknowledgements

This work was supported by the National Science Council and Atomic Energy Council of the Republic of China (Taiwan) under Contract Nos. NSC-90-2623-7-008-006-NU and NSC 91-2623-7-008-001-NU.

References

1. W. F. SMITH, in "Structure and Properties of Engineering Alloys," 2nd ed. (McGraw Hill, Inc., New York, 1993) p. 317.
2. I. BEN-HAROE, A. ROSEN and I. W. HALL, *Mater. Sci. Tech.* **9** (1993) 620.
3. R. AYER, C. F. KLEIN and C. N. MARZINSKY, *Metall. Trans.* A **23** (1992) 2455.
4. J. HICKLING and N. WIELING, *Corrosion* **37** (1981) 147.
5. D. P. SCHWEINSBERG, B. SUN and V. OTIENO-ALEGO, *J. Appl. Electrochem.* **24** (1994) 803.
6. D. P. SCHWEINSBERG, B. SUN, M. CHENG and H. FLITT, *ibid.* **23** (1993) 1097.
7. *Idem.*, *Corrosion Sci.* **36** (1994) 361.
8. W. TYSON, *Metall. Trans.* A **15** (1984) 1475.
9. P. ROZENAK and D. ELIEZER, *Mater. Sci. Eng.* **61** (1983) 31.
10. *Idem.*, *Metall. Trans.* A **20** (1989) 2187.
11. P. ROZENAK, *J. Mater. Sci.* **25** (1990) 2532.
12. D. N. GLADWIN, R. H. PRIEST and D. A. MILLER, *Mater. Sci. Tech.* **5** (1989) 40.
13. B. A. SENIOR, *Mater. Sci. Eng.* A **130** (1990) 51.
14. B. A. SENIOR, J. MAGUIRE and C. A. EVANS, *ibid.* **138** (1991) 103.
15. S. R. ORTNER and C. A. HIPPSLEY, *Mater. Sci. Tech.* **8** (1992) 883.
16. *Idem.*, *ibid.* **11** (1995) 998.
17. "ASM International Handbook Committee," in "Metals Handbook, 10th ed., Vol. 1, Properties and Selection: Irons, Steels, and High-Performance Alloys" (ASM International, Materials Park, OH, USA, 1990) p. 870.
18. C.-K. LIN and S.-T. YANG, *Eng. Fract. Mech.* **59** (1998) 779.
19. J. R. DAVISS, "Corrosion: Understanding the Basics" (ASM International, Materials Park, OH, USA, 2000) p. 427.
20. K. J. MILLER and R. AKID, *Proc. R. Soc. Lond.* A **452** (1996) 1411.
21. C.-K. LIN and W.-J. TSAI, *Fatigue Fract. Eng. Mater. Struct.* **23** (2000) 489.
22. C.-K. LIN, W.-C. FAN and W.-J. TSAI, *Corrosion* **58** (2002) 904.
23. C. LAIRD and D. J. DUQUETTE, in "Corrosion Fatigue: Chemistry, Mechanics and Microstructure," edited by O. Devereux, A. J. McEvily and R. W. Staehle (National Association of Corrosion Engineers, Houston, USA, 1972) p. 88.
24. D. J. MCADAM, *Proc. ASTM* **26** (1926) 224.
25. R. P. WEI and M. GAO, in "Hydrogen Effects on Mechanical Behavior," edited by N. R. Moody and A. W. Thompson (The Minerals, Metal and Materials Society, Warrendale, PA, USA, 1990) p. 789.
26. S. SURESH, G. F. ZAMISKI and R. O. RITCHIE, *Metall. Trans.* A **12** (1981) 1435.
27. S. SURESH, A. K. VASUDEVAN and P. E. BRETZ, *ibid.* **15** (1984) 369.
28. B. F. BROWN, C. T. FUJII and E. P. DAHLBERG, *J. Electrochem. Soc.* **116** (1969) 218.
29. G. SANDOZ, C. T. FUJII and B. F. BROWN, *Corrosion Sci.* **10** (1970) 839.

Received 3 December 2003
and accepted 23 June 2004